BLADE ELEMENT MOMENTUM SIMULATIONS USING POLARS EXTRACTED FROM WIND-TURBINE-MODEL EXPERIMENTS

Pedro Trombini Rodrigues
UNESP - São Paulo State University, Av. Profa Isette Correa Fontão, 505, São João da Boa Vista, SP 13876-750, Brazil
pedro.trombini@unesp.br
Diego Magela Lemos
University of São Paulo, Av. Trabalhador São Carlense, 400, São Carlos, SP 13566-590, Brazil
diegomagela@usp.br
Carlos do Carmo Pagani, Jr.
UNESP - São Paulo State University, Av. Profa Isette Correa Fontão, 505, São João da Boa Vista, SP 13876-750, Brazil
c.pagani@unesp.br
Daniel Sampaio Souza
UNESP - São Paulo State University, Av. Profa Isette Correa Fontão, 505, São João da Boa Vista, SP 13876-750, Brazil
daniel.s.souza@unesp.br

Abstract. *Due to rotational effects, the observed load of inboard sections of rotary wings is consistently higher than the load predicted based on the two-dimensional aerodynamic behavior of the corresponding airfoil in linear motion. Therefore, engineering methods used to analyze and optimize the aerodynamics of horizontal-axis wind turbines (HAWT) rely on corrections to 2D airfoil data. Since the physics associated with the phenomenon is not fully understood, the correction models have to resort to empirically determined parameters. It is important to stress that a great scattering of the turbine power predictions based on different correction models is observed for conditions of high blade load. We propose a methodology to predict the load on HAWT blades based on the widely applied blade element momentum (BEM) method that does not rely on the correction of 2D polar curves. In the proposed methodology, the force coefficients are stored in the lookup table and consulted by the BEM algorithm, not only as function of the angle of attack but also as function of the chord-to-radius ratio and the local Rossby number. The data of the lookup table is provided by the measurements of the unsteady aerodynamic experiment Phase-VI, coordinated by the United States' National Renewable Energy Laboratory and conducted in a 24.4m×36.6m wind tunnel in NASA Ames Research Center. Compared to a well accepted correction model, the proposed methodology predict the load radial distribution with greater accuracy for relatively high wind speeds.*
Keywords: *Wind turbine, rotational augmentation, Blade Element Momentum.*

1. INTRODUCTION

The blade element momentum (BEM) method is one of the most regularly employed tool for horizontal-axis-wind-turbine (HAWT) aerodynamic predictions, both for analysis and design proposes. It is based on Froude's momentum theory and assumes the flow over each blade section to be independent. In principle, the load on a particular section is assumed to be the same of a section of the same profile shape in two-dimensional flow, at the same angle of attack (α) and chord-based Reynolds number (Re). This approximation is reasonable for low to moderate angles of attack. However, as separation starts to occur, rotational effects enhance and the section flow becomes significantly different from that observed in 2D conditions (Du and Selig, 2000; Bangga *et al.*, 2017). In general, the lift force experienced by sections of rotating wings is larger than the one expected from two-dimensional experiments for the same angle of attack and Reynolds number, and the phenomenon is referred to as rotational augmentation.

At pre-stall angles of attack, the rotational effects are known to delay the first appearance of boundary-layer separation on rotating-wing sections to higher angles of attack (Banks and Gadd, 1963; Mauro *et al.*, 2017). This separation delay is due to the partial compensation of the adverse pressure gradient through the chord-wise component of the Coriolis force when the radial flow becomes significant (Du and Selig, 2000). However, the rotational augmentation is particularly effective in conditions for which a significant portion of the boundary layer is separated (Schreck *et al.*, 2007). In such conditions, the volume of the separated flow region over sections of rotating wings reduces significantly compared to what is observed in two-dimensional flow (Bangga *et al.*, 2017). Although this reduction is commonly attributed to spanwise drainage of the vorticity in the separated flow region, known as centrifugal pumping, investigation at conditions representative of fly wings showed that this effect is not sufficient to explain the stabilization of the leading-edge vortice (Wojcik and Buchholtz, 2014; Werner *et al.*, 2019). Moreover, there are recent evidences that for wind-turbine sections, mechanisms other than the centrifugal pumping may significantly contribute to the volume reduction of the region of separated flow (Souza and Gennaro, 2020).

During a BEM computation, the lift and drag coefficients on each blade section are obtained by consulting lookup tables built from two-dimensional wind-tunnel measurements or numerical simulations. Semi-empirical models are commonly used to correct the force coefficients due to rotational effects. Several corretion methods have been proposed. Snel *et al.* (1993) proposed a correction for the lift coefficient based on the local chord-to-radius ratio c/r. They adjusted parameters of the model based on comparisons between predictions for 2D and rotational flows over a wind-turbine section

performed by a viscous-inviscid interaction code. Chaviaropoulos and Hansen (2000) on the other hand used comparisons between Navier-Stokes computations for 2D and quasi-3D flows to adjust the parameters of a correction method for the lift, drag and pitching moment coefficients. Tafur *et al.* (2020) used Chaviaropoulos and Hansen's model with constants calibrated by simulations with computational fluid dynamics (CFD). Bak *et al.* (2006) proposed a model to correct the difference between the pressure on the suction and pressure side of the blade section. The correction function was a product of an amplification and a shape function, adjusted to match results of CFD simulations with the NREL Phase-VI measurements (Hand *et al.*, 2001). Dowler and Schmitz (2015) proposed a model for which the corrections depend on the radial distribution of circulation, demanding an iterative method, and constants adjusted based on experimental data.

Breton *et al.* (2007) compared some correction models, including some of the aforementioned. In comparison to wind-tunnel measurements by Hand *et al.* (2001), the models in general overpredicted the blade loads in conditions of high wind velocity. Moreover, Breton *et al.* (2007) evidenced a significant scattering of the predictions. The observed scattering is probably due to the lack of a complete understanding about the physics of the rotational augmentation, which results in different sets of assumptions and the need to resource to empirical parameters that are adjusted based on data for a particular geometry and specific operational conditions. The work described here proposes a BEM methodology which, instead of applying corrections to 2D data, consults the aerodynamic coefficients from an enhanced lookup table referenced by the sectional angle of attack and additional non-dimensional parameters related to the rotational effects.

The paper is organized as follows. Section 2 describes the adopted methodology including the presentation of the widely-used BEM method and a modified version proposed by the authors, which involves building a lookup table to store the relevant parameters for a particular airfoil and experiments conditions. This section also presents how the experimental data were obtained as well as the corrections applied. Section 3 shows the results achieved based on the XFOIL data and BEM method using enhanced data, which were compared with experiments of reference. Finally, Section 4 provides conclusions and highlights the potential of the methodology presented here.

2. METHODOLOGY

2.1 Blade Element Momentum method

The BEM method combines the momentum theory for an ideal actuator disc with the characteristics of two-dimensional flow around an airfoil. The momentum theory applies to both motor rotors (helicopter and propulsion propellers) and generator rotors (windmills and wind turbines). It is considered a streamtube that has one of its sections coinciding with the rotor and applies a thrust force T on the fluid passing through it. Assuming steady flow, incompressible and non-viscous conditions at upstream and downstream locations from the rotor plane, it can be shown that

$$T = 2\pi\rho V_0^2 \underline{a}(1-\underline{a})\Re^2, \tag{1}$$

where V_0 is the wind velocity, $\Re$ is the radius of the rotor and $\underline{a}$ is the axial induction factor, defined by the relation

$$V = (1-\underline{a})V_0, \tag{2}$$

where V is the velocity in the rotor plane. The method assumes that the flow over each blade section is independent of the flow in the other sections. Therefore, it is convenient to consider the contribution of an annular region of width dr at a distance r from the rotor axis,

$$dT = 4\pi\rho V_0^2 \underline{a}(1-\underline{a})r dr. \tag{3}$$

In Fig. 1(a), we consider two alternative forms of decomposition of the force per unit span applied on a section of the blade, while Fig. 1(b) describes the relative velocity V_{rel} observed by a frame of reference fixed to the section. It is observed that, in addition to V_0, V_{rel} depends on the rotational speed Ωr, the radial induction factor and the tangential induction factor a'. Defining $C_{th} = C_l\cos\phi + C_d\sin\phi$, where C_{th} is the thrust coefficient, C_l and C_d are the lift and drag coefficients, respectively, we obtain the contribution of a strip of width dr of the rotor to the thrust force as

$$dT = \frac{1}{2}\rho B\frac{V_0^2(1-\underline{a})^2}{\sin^2\phi}cC_{th}dr, \tag{4}$$

where c is the chord of the considered section and B is the number of rotor blades. Equating Eqs. 3 and 4, we obtain a relation for the axial induction factor as

$$\underline{a} = \frac{cBC_{th}}{8\pi r\sin^2\phi + cBC_{th}}. \tag{5}$$

Tangential induction is the result of the reaction to the moment caused by the fluid over the rotor blades. Considering a control volume given by an annular streamtube of width dr passing through the rotor at a distance r from the shaft, it can be shown that the rate of angular momentum transport to the fluid is given by

$$dQ = 4\pi\rho\Omega V_0 a'(1-a')r^3 dr. \tag{6}$$

Comparing with the axial component of the torque due to the forces acting on the blade section, a relation for the tangential induction factor is obtained as

$$a' = \frac{cBC_q}{8\pi r \sin\phi\cos\phi - cBC_q}, \tag{7}$$

where $C_q = C_l \sin\phi - C_d \cos\phi$ is the aerodynamic force coefficient in the tangential direction to the rotor plane (see Fig. 1(a)). The method is iterated until a solution that balances the aerodynamic forces in each section with the induction factors is reached. During an iteration cycle, the method requires the values of the aerodynamic coefficients for a given angle of attack that depend on the blade geometry, through θ, and the induction factors, through ϕ and the absolute value of V_{rel} (see Fig. 1(b)). These coefficients are commonly obtained from a lookup table generated from two-dimensional experiments or simulations.

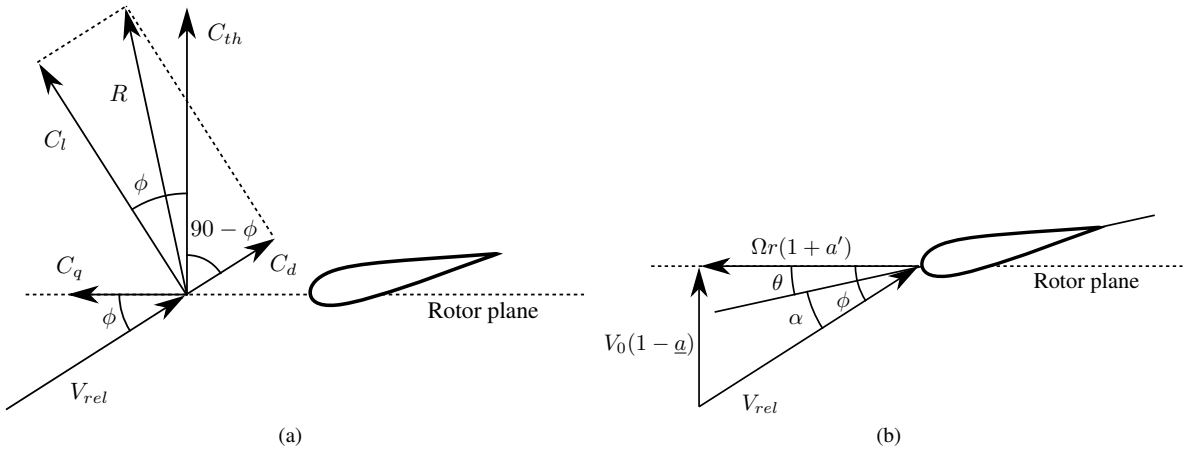

Figure 1. (a) Two alternative aerodynamic force decomposition forms on a blade section and (b) flow velocity according to a reference frame attached to a blade section. Adapted from Hansen (2008).

A version of the basic algorithm for the BEM method proposed by Hansen (2008) was implemented in MATLAB® scripting language. Originally, the code was based on force coefficients obtained by two-dimensional simulations performed with XFOIL (Drela, 1989) and the extrapolation method by Viterna and Corrigan (1982) for high angles of attack. The code features also the Prandtl tip loss correction, which takes into account the finite number of blades, and a correction for high axial induction.

2.2 BEM with enhanced lookup table

Neglecting the influence of neighboring sections, the flow over a particular blade section distant r from the rotor axis depends on c/r, α, local Rossby number $Ro = V_\infty/(\Omega c)$ and $Re = V_\infty c/\nu$, where V_∞ is the local free-stream velocity, Ω is the rotor angular speed, and ν is the air kinematic viscosity. However, for some conditions the effect of the Reynolds number may be negligible (Mauro *et al.*, 2017). Based on this dimensional argument, a BEM-based methodology is proposed in which the lift and drag coefficients are stored as functions of α, c/r and Ro in the lookup table. During the processing, normal and tangential coefficients are obtained according to the local values for these parameters. For this, the data must be obtained from experiments or simulations for rotating configurations. In the work described here, we used polar data extracted from the unsteady Phase-VI experiment campaign performed by the National Renewable Energy Laboratory (NREL) (Hand *et al.*, 2001) (see Sec. 2.3). The measurements of sequence H for wind speeds of 5, 7, 10, 15, 20m/s were used and the sectional angle of attack was corrected according to Sant *et al.* (2006).

It is important to note that the sectional flow dependence on α, c/r and Ro can equivalently be represented as a dependence on α, c/r and θ. Therefore, the proposed methodology is in some sense similar to Chaviaropoulos and Hansen's one. The difference is that the present one accounts for the rotational effects without the need of empirically determined coefficients. The advantage is that no adjustment of the empirical coefficients is required for a particular airfoil

geometry. On the other hand, the methodology demands a number of wind-tunnel experiments or, alternatively, numerical simulations of a turbine rotor to build the lookup table of each airfoil.

2.3 Wind-turbine experimental model

The reference experimental data consist of measurements of the unsteady aerodynamic experiment Phase-VI, carried out by the American National Renewable Energy Laboratory (NREL) in a wind tunnel with a test section of 24.4m×36.6m (80ft×120ft) in NASA Ames Research Center (Hand *et al.*, 2001). The set of measurements chosen for the present analysis is identified here as H sequence, according to the nomenclature given by Hand *et al.* (2001). This test sequence used an upwind, rigid turbine with a 0° cone angle. Blade and probe pressure measurements were collected under conditions where the wind speed ranged from 5m/s to 25m/s. Table 1 shows the rotor characteristics used in the experiment for H sequence.

Table 1. Rotor geometry and operation data for the data considered here.

Basic characteristics of the rotor			
Blade profile	–	NREL S809	–
Blade tip pitch angle	β_t	3	°
Yaw angle	ψ	0	°
Number of blades	B	2	–
Sectional Reynolds number	Re	$(0.6 \sim 1.2)\times 10^6$	–
Rotor angular speed	Ω	72	RPM
Rotor radius	$\Re$	5.029	m

In the NREL Phase-VI experiments, flow direction 5 hole probes were installed upon a rod ahead of the leading edge of the blade in order to measure the local flow angle (LFA) (see Fig. 2). Nonetheless, it is worth to highlight that even using a rod the probes were still in a region influenced by the bound circulation of the blade. Thus, a correction has to be applied in this technique to be able to estimate the angle of attack from the measured local flow angle (Sant *et al.*, 2006). Thereby, Sant *et al.* (2006) proposed a method in which a free wake vortex model is used to derive a estimated distribution for the sectional angle of attack for the NREL Phase-VI wind turbine under different operating conditions. The method is based on the detailed blade surface pressure measurements. Moreover, the results presented in Sant *et al.* (2006) were used to corrected the experimental data for the local (sectional) angle of attack from experiments and to build the lookup table as well.

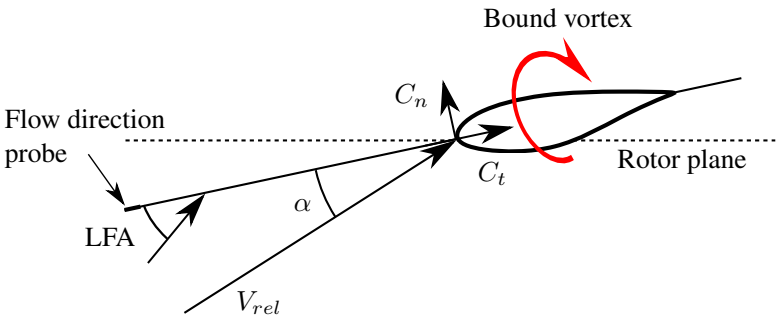

Figure 2. Blade section aerodynamic load coefficients together with schematic representation of the probe location installed to measure the local flow angle (LFA). Adapted from Sant *et al.* (2006).

Reference velocities of 5, 7, 10, 13, 15, 17, 20m/s were then selected to compose our analysis, considering the yaw angle equal to 0°. Lift and drag coefficients of the lookup table were obtained by proper transformation of the measured normal and tangential force coefficients for the reference wind speeds of 5, 7, 10, 15, 20m/s available in H sequence considering the corrected angle of attack distribution proposed by Sant *et al.* (2006). These coefficients are defined as normal (C_n) and tangential (C_t) to the local chord (see Fig. 2). The proposed BEM methodology was used to predict the blade loads for the reference wind speeds as well as for two additional wind speeds, namely V_0 = 13m/s and 17m/s.

3. RESULTS

Figures 3 to 6 show the numerical and experimental results to the radial distributions for the corrected angle of attack associated to each considered wind speed. From the figures, it is observed a good agreement between the BEM method

based on experimental data and the corrected experimental results, especially in mid sections. In comparison to the BEM method based on the XFOIL data, the model proposed here performed better, particularly at the root region at high wind speeds, for which intense rotational effects are expected. Both methods underpredicted the angle of attack at the blade tip, although the proposed method performed slightly better. Differences between the measurements and predictions may be attributed to a significant local influence of tip vortex. Furthermore, the combined effect from three-dimensionalities and rotation are equally important and contributes to deviations. Since corrected angles of attack were not available in Sant *et al.* (2006) for V_0 = 17m/s, the predicted values were not compared to the measurements for this speed.

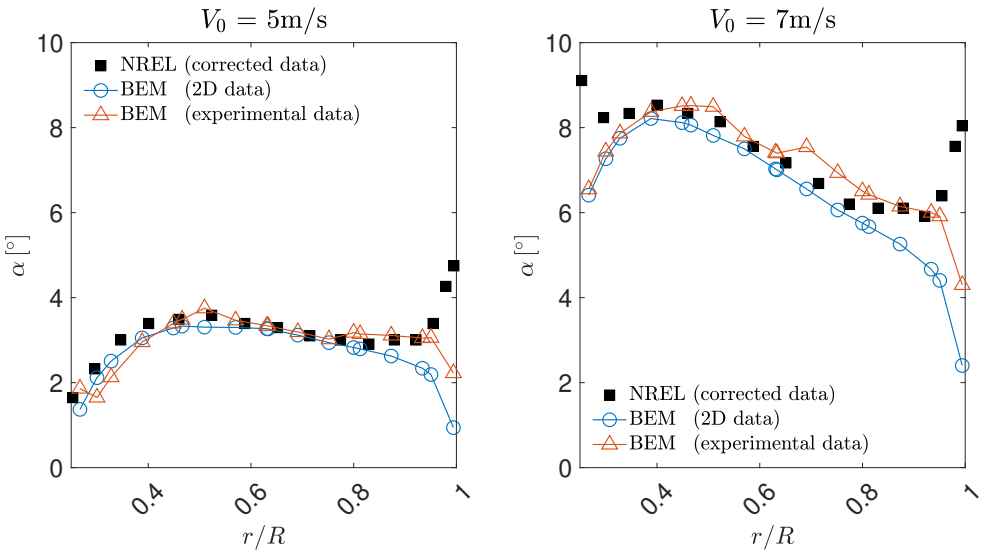

Figure 3. Angle of attack distribution along radial position considering wind speed V_0 equals to 5m/s and 7m/s.

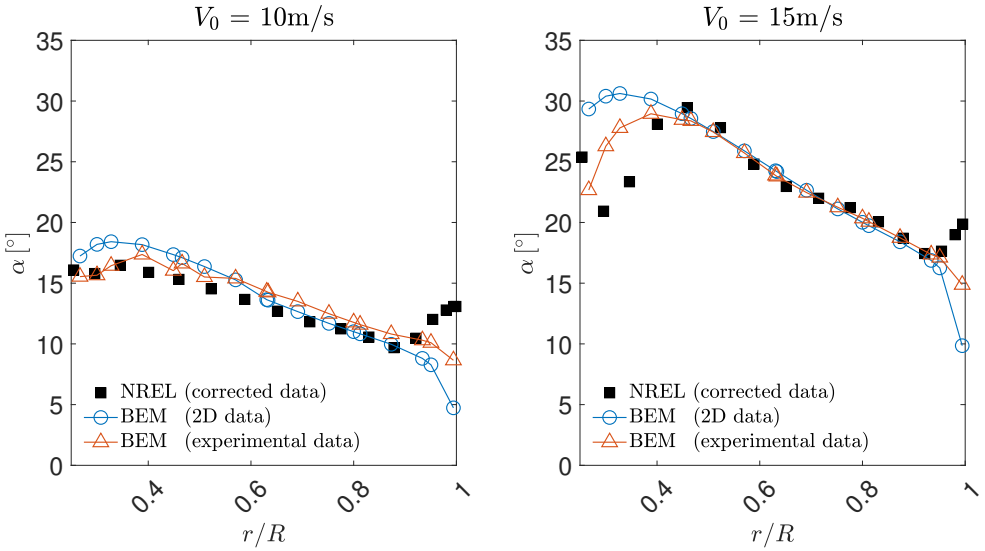

Figure 4. Angle of attack distribution along radial position considering wind speed V_0 equals to 10m/s and 15m/s.

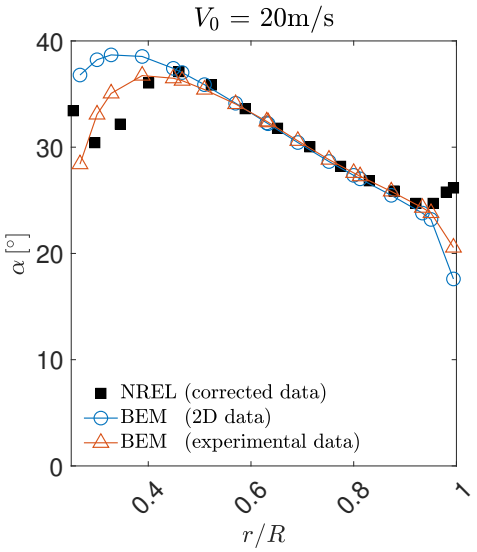

Figure 5. Angle of attack distribution along radial position considering wind speed V_0 equals to 20m/s.

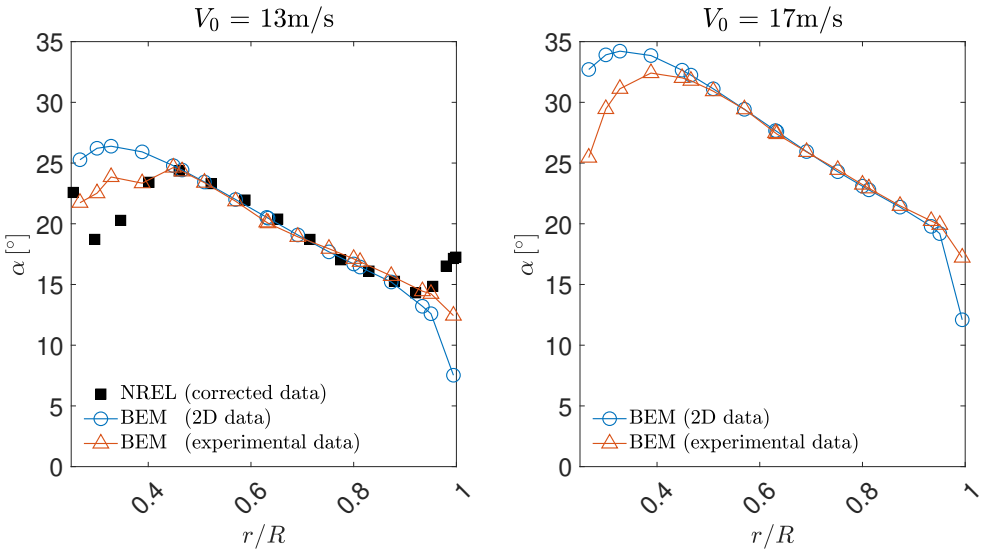

Figure 6. Angle of attack distribution along radial position considering wind speed V_0 equals to 13m/s and 17m/s.

Figures 7 to 13 illustrate the numerical and experimental results for the normal and tangential force coefficients. The experimental coefficients were obtained based on the pressure distribution on selected sections. In order to establish a quantitative analysis for the results, a fit metric based on the normalized mean square error (NMSE) was employed. Its formulation is defined as

$$\text{NMSE} = \frac{\overline{(C_o - C_p)^2}}{\bar{C}_o \bar{C}_p}, \tag{8}$$

where C_o and C_p are, respectively, reference and predicted data sets, while the overbar indicates the mean over the sampling points. The reference data used in this approach correspond to the experimental measurements and, to obtain coefficient predictions at the same radial positions where they were measured, interpolation between neighboring sections

was applied.

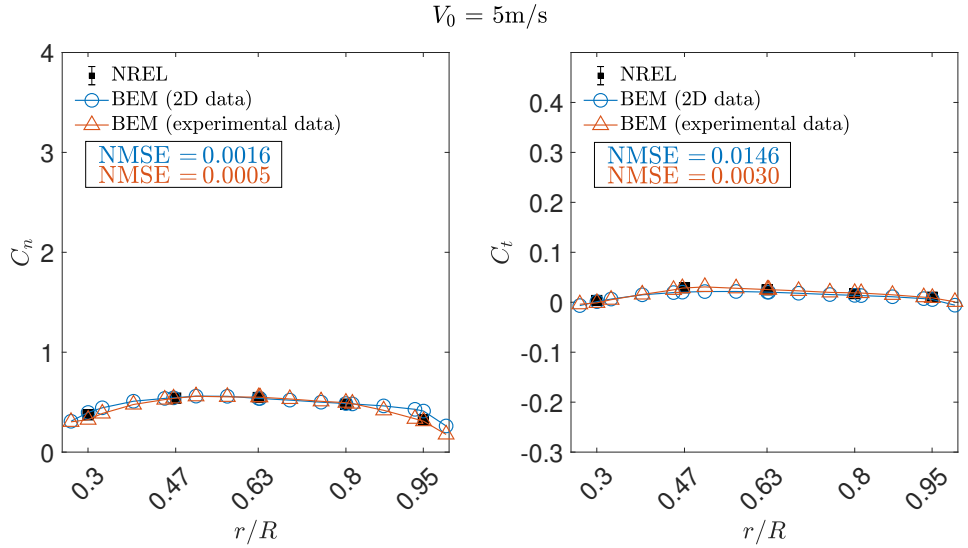

Figure 7. Radial distribution for the normal and tangential force coefficients considering wind speed V_0 equals to 5m/s.

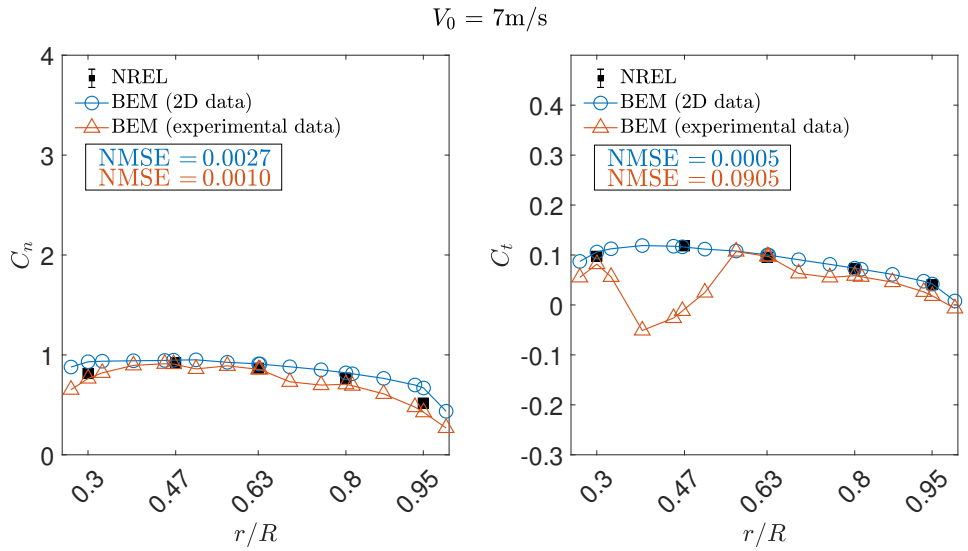

Figure 8. Radial distribution for the normal and tangential force coefficients considering wind speed V_0 equals to 7m/s.

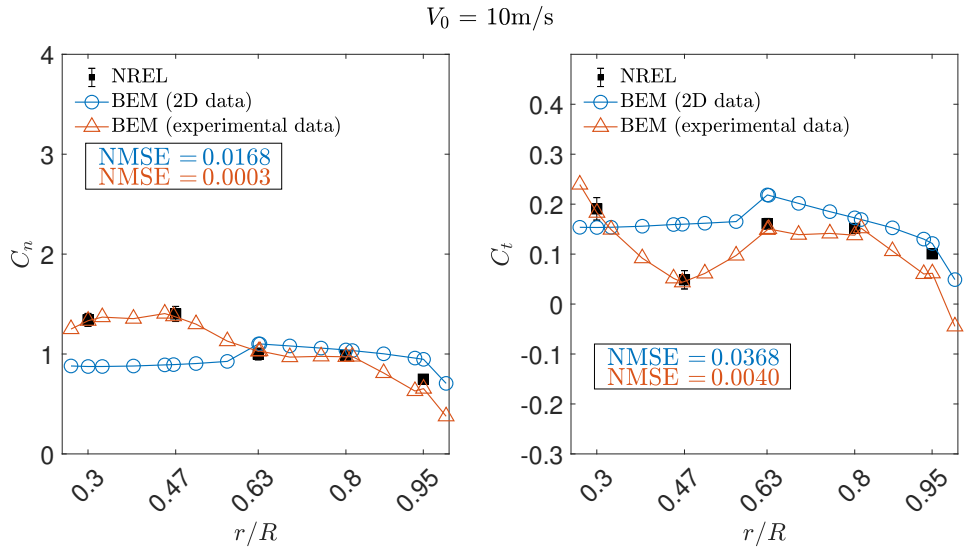

Figure 9. Radial distribution for the normal and tangential force coefficients considering wind speed V_0 equals to 10m/s.

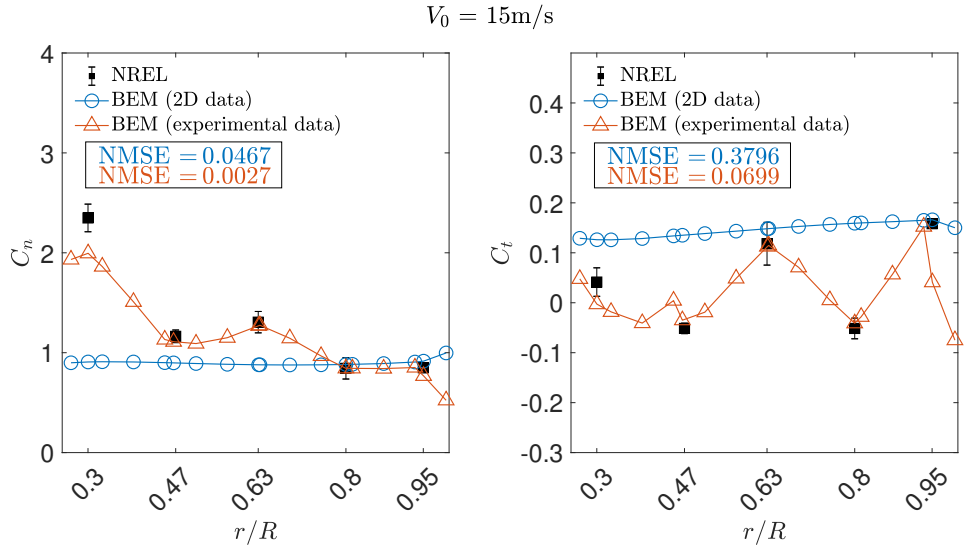

Figure 10. Radial distribution for the normal and tangential force coefficients considering wind speed V_0 equals to 15m/s.

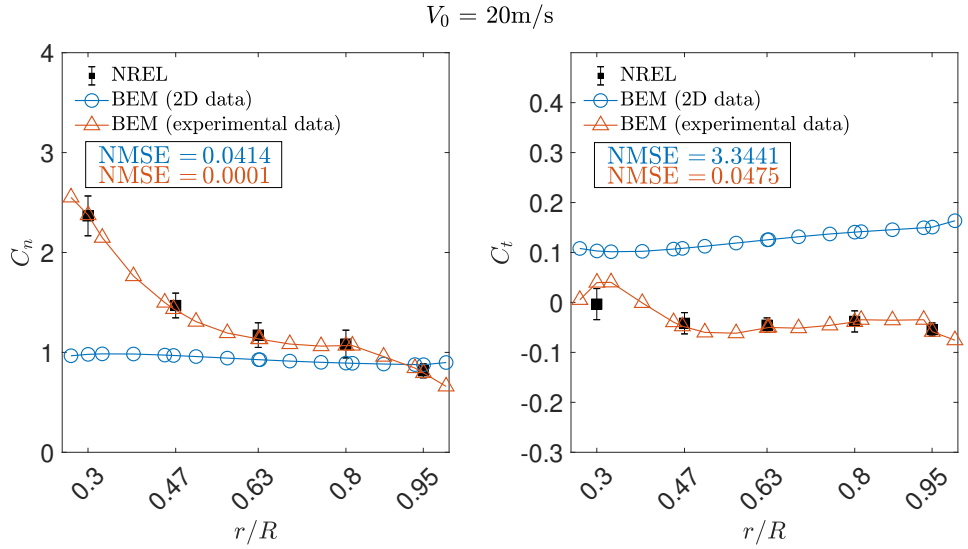

Figure 11. Radial distribution for the normal and tangential force coefficients considering wind speed V_0 equals to 20m/s.

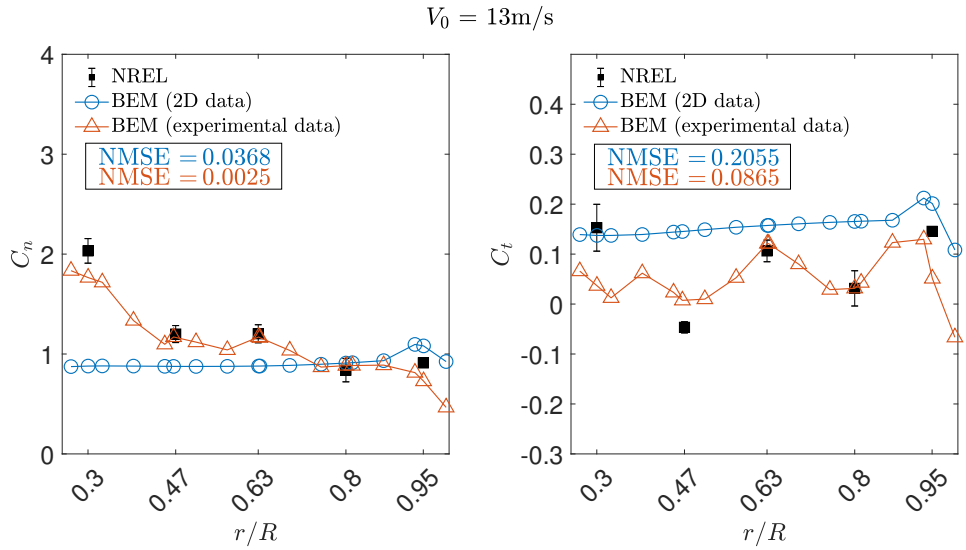

Figure 12. Radial distribution for the normal and tangential force coefficients considering wind speed V_0 equals to 13m/s.

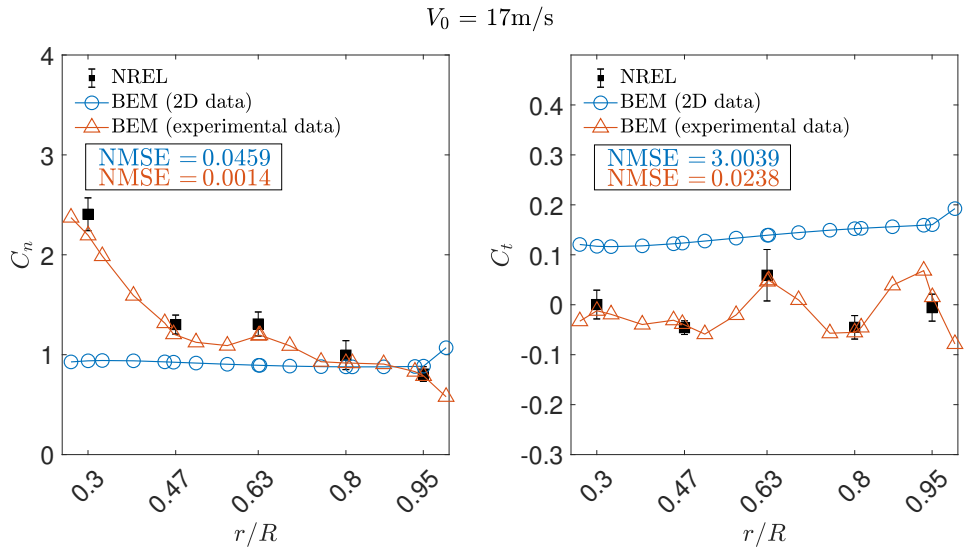

Figure 13. Radial distribution for the normal and tangential force coefficients considering wind speed V_0 equals to 17m/s.

From the figures, it can be noted that, for the same radial position, the normal force coefficient increased when the velocity is increased, while the tangential force coefficient varied between positive and negative values. It is also observed that higher velocities tended to have the greatest standard deviations as a result of the greater influence of unsteadiness present mainly in regions of separated boundary layer.

It is important to highlight that for the velocity of 5m/s there was a good approximation between the coefficients indirectly measured by the experiment and those calculated by both BEM method using XFOIL-based data and the method using the enhanced lookup table. For wind speeds greater than 7m/s, there was a weaker convergence for the results for the BEM method with XFOIL data and a good fit for the BEM method using enhanced data. Exceptionally for V_0=7m/s, the proposed model did not predict C_t accurately between r/R=0.30 and ≈ 0.57. The reason for that is not clear, since the method improved the prediction in comparison to the reference BEM simulations for the C_n at the same speed and radial position, and further investigation is needed.

Other factors besides the local Rossby number and chord-to-radius ratio may play an important role for the observed difference between the flow over a blade section and the flow over the corresponding airfoil in 2D motion, such as three-dimensional effects, e.g. the interaction of neighboring section and blade-tip effects. These effects are inherently accounted for in the table based on the Ro and c/r for the particular case from which the data were obtained. However, since the 3D effects may depend on the blade geometry and operational condition, the enhanced lookup table might not be adequate to predict the load for shapes or conditions different from the ones used to collect its data. The fact that the load predicted by the proposed model agreed well with the experiments for the cases with V_0=13 and 17m/s, whose data were not used to feed the lookup table, suggests that, at least within certain operational range, the methodology might be

of practical interest. Nevertheless, further tests should be performed, preferably with blades of different planar shape.

Figure 14 shows the resultant torque for the entire blade in analysis comparing with the experimental data and the free-wake model proposed by Sant *et al.* (2006). The corrected experimental data measured from low-speed shaft torque, referred as LSSTQCOR, and the estimated aerodynamic torque (EAEROTQ), according to the nomenclature by Hand *et al.* (2001), are presented. Referred to the LSSTQCOR measurements, the method proposed here had a level of agreements similar to the BEM based on XFOIL data for high wind speeds, but underpredicted the torque instead of overpredicting it. Taking the EAEROTQ as reference, the present model performed better predictions than the XFOIL-based method. Note that the present computation agreed well with the free-wake predictions by Sant *et al.* (2006).

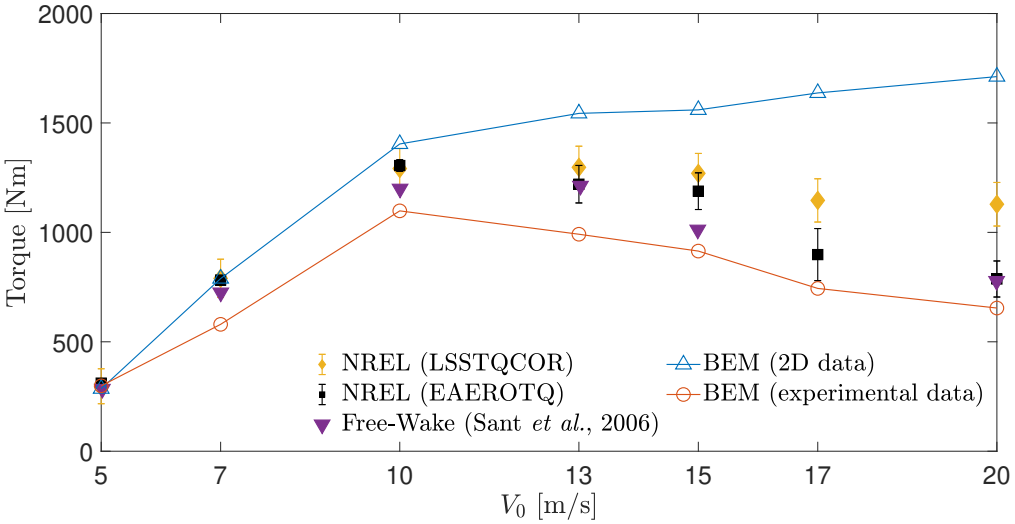

Figure 14. Variation in torque with wind speed comparing BEM methods results with experimental data considering the corrected low-speed shaft torque (LSSTQCOR) and the estimated aerodynamic torque (EAEROTQ). The free-wake model proposed by Sant *et al.* (2006) is also shown.

4. CONCLUSIONS

A variation of the blade element momentum method is proposed for the prediction of aerodynamic loads of horizontal-axis wind turbines. The methodology does not feature empirical modeling for the correction of the aerodynamic coefficients. Instead it is proposed to use a lookup table in which the coefficients are stored as functions of the angle of attack, chord-to-radius ratio and sectional Rossby number. The data for the table were obtained from wind-tunnel experiments carried out for a 10m-diameter wind-turbine model. Compared to a widely-used approach, the proposed methodology showed a significant accuracy improvement for relatively high wind speeds, for which rotational effects are expected to be relevant. Further tests are needed to investigate the effect of the particular blade planform and operational condition on the lookup table data. However, the method seems to represent a viable alternative to account for rotational effects in BEM computations without resourcing to empirically determined parameters.

5. ACKNOWLEDGEMENTS

P.T.R. received funding under grant #2020/10972-3, São Paulo Research Foundation (FAPESP). The authors are also grateful to Dr. Scott Schreck for providing the experimental data.

6. REFERENCES

Bak, C., Johansen, J. and Andersen, P., 2006. "Three-dimensional corrections of airfoil characteristics based on pressure distributions". In *European Wind Energy Conference Proceedings*. Athens, Greece.

Bangga, G., Lutz, T., Jost, E. and Krämer, E., 2017. "CFD studies on rotational augmentation at the inboard sections of a 10MW wind turbine rotor". *Journal of Renewable and Sustainable Energy*, Vol. 9, pp. 1–28.

Banks, W. and Gadd, G., 1963. "Delaying effect of rotation in laminar separation". *AIAA Journal*, Vol. 1, pp. 941–942.

Breton, S., Coton, F. and Moe, G., 2007. "A study on rotational effect and different stall delay models using a prescribed wake vortex scheme and NREL phase VI experiment data". *Wind Energy*, Vol. 11, pp. 459–482.

Chaviaropoulos, P. and Hansen, M., 2000. "Investigating three-dimensional and rotational effects on wind turbine blades

by means of quasi-3D Navier-Stokes solver". *Journal of Fluids Engineering*, Vol. 122, pp. 330–336.

Dowler, J. and Schmitz, S., 2015. "A solution-based stall delay model for horizontal-axis wind turbines". *Wind Energy*, Vol. 18, pp. 1793–1813.

Drela, M., 1989. "XFOIL: An analysis and design system for low reynolds number airfoils". In T. Mueller, ed., *Low Reynolds Number Aerodynamics*, Springer, Berlin, Heidelberg, Vol. 54.

Du, Z. and Selig, M., 2000. "The effect of rotation on the boundary layer of a wind turbine". *Renewable Energy*, Vol. 20, pp. 167–181.

Hand, M., D., S., Fingersh, L., Jager, D., Cotrell, J.R. Schreck, S. and Larwood, S., 2001. "Unsteady arodynamics experiment phase VI: Wind tunnel test configuration and available data campaigns". Technical report, NREL.

Hansen, M.O.L., 2008. *Aerodynamics of wind turbine*. Earthscan, London.

Mauro, S., Lanzafame, R. and Messina, M., 2017. "An insight into the rotational augmentation on HAWTs by means of CFD simulations - PART II: Post processing and force analysis". *International Journal of Applied Engineering Research*, Vol. 12, No. 21, pp. 10505–10529.

Sant, T., van Kuik, G. and van Bussel, G.J.W., 2006. "Estimating the angle of attack from blade pressure measurements on the NREL phase VI rotor using a free wake vortex model: Axial conditions". *Wind Energy*, Vol. 9, No. 6, p. 549–577.

Schreck, S., Soerensen, N. and Robinson, M., 2007. "Aerodynamic structures and processes in rotationally augmented flow fields". *Wind Energy*, Vol. 10, pp. 159–178.

Snel, H., Houwink, R., Bussel, G. and Bruining, A., 1993. "Sectional prediction of 3d effects for stalled flow on rotating blades and comparison with measurements". In *European Wind Energy Community Conference Proceedings*. Lübeck-Travemünde, Germany.

Souza, D. and Gennaro, E., 2020. "Rotational effects on the spanwise periodic flow over a wind turbine airfoil". In *18th Brazilian Congress of Thermal Sciences and Engineering*. Bento Gonçalves, Brazil.

Tafur, B., Daniele, E., Stoevensandt, B. and Thomas, P., 2020. "On the calibration of rotational augmentation models for wind turbine load estimation by means of cfd simulations". *Acta Mechanica Sinica*, Vol. 36, No. 2, pp. 306–319.

Viterna, L. and Corrigan, R., 1982. "Fixed pitch rotor performance of large horizontal axis wind turbines". Technical report, NASA.

Werner, N., Chung, H., Wang, J., Liu, G., Cimbala, J., Dong, H. and Cheng, B., 2019. "Radial planetary vorticity tilting in the leading-edge vortex of revolving wings". *Physics of Fluids*, Vol. 31, pp. 1–15.

Wojcik, C. and Buchholtz, J., 2014. "Vorticity transport in the leading-edge vortex on a rotating blade". *Journal of Fluid Mechanics*, Vol. 743, pp. 249–261.

7. RESPONSIBILITY NOTICE

The authors are solely responsible for the printed material included in this paper. The opinions, hypotheses and conclusions or recommendations expressed in this material are the responsibility of the authors and do not necessarily reflect the views of FAPESP.